# Techno-Economic Analysis of a PV-Battery Water Pumping Microgrid System for Off-Grid Rural Communities in the United States: Case Study of the Navajo Nation

by

**Aryana Y. Nakhai**

B.S. Electrical Engineering, University of Pittsburgh, 2018

Submitted to the Graduate Faculty of the

Swanson School of Engineering in partial fulfillment

of the requirements for the degree of

Master of Science in Electrical and Computer Engineering

University of Pittsburgh

2020

UNIVERSITY OF PITTSBURGH

SWANSON SCHOOL OF ENGINEERING

This thesis was presented

by

**Aryana Y. Nakhai**

It was defended on

November 2, 2020

and approved by

Dr. Alexis Kwasinski, PhD., Associate Professor,
Department of Electrical and Computer Engineering

Dr. Robert J. Kerestes, PhD., Assistant Professor,
Department of Electrical and Computer Engineering

Dr. Brandon M. Grainger, PhD., Assistant Professor,
Department of Electrical and Computer Engineering

Thesis Advisor: Dr. Alexis Kwasinski, PhD., Associate Professor,
Department of Electrical and Computer Engineering

**Techno-Economic Analysis of a PV-Battery Water Pumping Microgrid System for Off-Grid Rural Communities in the United States: Case Study of the Navajo Nation**

Aryana Y. Nakhai, M.S.

University of Pittsburgh, 2020

Lack of access to running water has been a pressing issue in many developing countries across the world; however, it is also a problem in the United States. Today, more than two million Americans living in rural areas lack access to basic water supply and infrastructure. Rural communities tend to be located in environmentally fragile areas with poor economic conditions, making access to appropriate, low-cost technology for clean water supply and sanitation more challenging. In addition, many of the water resources located in these areas are being jeopardized by climate change in recent years. This research proposes a photovoltaic (PV)-battery microgrid system for powering water pumps in off-grid areas in efforts to identify an economical and technologically feasible solution to the water issues faced by these communities. Utilizing the HOMER Pro software, developed by the U.S. National Renewable Energy Laboratory (NREL), the case of the Navajo Nation is examined by analyzing the effects of this region's air temperature on the life and performance of battery storage and the economics of the proposed microgrid system. This research is intended to serve as a guide for rural off-grid communities in addressing their pressing water availability crisis, which is even more exacerbated by the erosion of surface water flows due to climate change.

## Table of Contents


**Acknowledgments** ........ x

**1.0 Introduction** ........ 1

**2.0 PV-Battery Water Pumping** ........ 5

  **2.1 Technology & Operation** ........ 5

  **2.2 System Parameters** ........ 6

**3.0 The Case of the Navajo Nation** ........ 11

  **3.1 Water Accessibility** ........ 12

  **3.2 Water Availability & Climate Change** ........ 13

**4.0 System Design & Sizing** ........ 17

  **4.1 Battery Storage** ........ 20

  **4.2 System Sizing** ........ 22

    **4.2.1 Technical & Economic Assumptions** ........ 23

    **4.2.2 Quantitative Results** ........ 26

    **4.2.3 HOMER Pro Simulation** ........ 30

      **4.2.3.1 Simulation Inputs** ........ 30

      **4.2.3.2 Simulation Results** ........ 36

**5.0 Economic Analysis** ........ 38

  **5.1 Effects of Temperature on System Costs** ........ 38

  **5.2 PV-Diesel vs. PV-Battery Systems** ........ 42

**6.0 Conclusion and Implications** ........ 45

**Appendix A Solar Radiation Data** ........ 48

**Appendix B Projections of Monthly Temperatures ........................................................ 49**

**Appendix C HOMER Pro Results ..................................................................................... 50**

**Bibliography ...................................................................................................................... 51**

## List of Tables


**Table 1 Projected Temperature Increases by 2050 .......... 22**

**Table 2 Assumptions for Proposed System .......... 23**

**Table 3 Assumptions for PV Panels .......... 24**

**Table 4 Assumptions for Battery Storage .......... 25**

**Table 5 Assumptions for System Operation .......... 26**

**Table 6 Summary of Quantitative Results for System Sizing .......... 29**

**Table 7 Summary of Simulation Results .......... 37**

**Table 8 Estimated Units of Replacements and O&M Costs for System Components .......... 39**

**Table 9 System Costs under Pessimistic Scenario – w/ Temperature Effects .......... 39**

**Table 10 System Costs under Pessimistic Scenario – w/o Temperature Effects .......... 40**

**Table 11 Battery Storage Sizing and Costs (Mean Values) .......... 41**

**Table 12 Assumptions for Diesel Generator .......... 42**

**Table 13 Cost Summary of Energy Storage Alternatives .......... 43**

**Table 14 Solar Radiation Data for Navajo Nation .......... 48**

**Table 15 Projected Monthly Temperatures in Navajo Nation by 2050 .......... 49**

**Table 16 Summary of Simulation Results – w/ Temperature Effects .......... 50**

**Table 17 Summary of Simulation Results - w/o Temperature Effects .......... 50**

## List of Figures

Figure 1 Solar Irradiance vs. Time of Day .................... 8
Figure 2 Total Dynamic Head Determination for a Water Well .................... 9
Figure 3 Map of the Five Agencies on the Navajo Nation .................... 11
Figure 4 Projected Changes in Average Annual Temperatures in Southwest U.S. .................... 14
Figure 5 Projected Changes in Spring Precipitation by Mid-21st Century .................... 14
Figure 6 Groundwater Aquifers in Navajo Nation's Western Agency .................... 16
Figure 7 Classification of PV Driven Motors .................... 17
Figure 8 Block Diagram of Proposed PV-Battery Water Pumping System .................... 19
Figure 9 Battery SOH and Charging Cycles at Different Temperatures .................... 20
Figure 10 Daily Load Profile .................... 25
Figure 11 HOMER Schematic of Proposed System .................... 31
Figure 12 HOMER Functional Model of Modified Kinetic Battery .................... 31
Figure 13 Relationship between Shelf Life and Temperature .................... 33
Figure 14 Relationship between DOD and Cycles to Failure .................... 34
Figure 15 Relationship between Temperature and Relative Capacity .................... 35
Figure 16 Cost Comparison between Energy Storage Alternatives .................... 43

*"The best way to predict the future is to create it."*

*– Peter F. Drucker*

# Acknowledgments

"*Poverty and peace cannot co-exist.*" I was about eight years old when I first read these words by James Wolfensohn, President of the World Bank (1995-2005), on the cover of one of my father's books. At that time, it really did not inspire any new thinking in me immediately. As I grew older and travelled to a number of Middle Eastern and Latin American countries and witnessed communities with varying degrees of hardship and poverty, it became increasingly evident to me how poverty and peace are related. Anytime I saw a poor neighborhood and people struggling in very poor conditions, I would imagine how I could help to improve their lives. As a student, my thoughts about fighting poverty and helping people soon inspired me to pursue my college education in engineering so that I could ultimately have a positive influence on society. I always had an interest in working towards creating new and innovative ways to impact lesser developed communities. This research is a reflection of my passion for renewable energy technologies and the opportunities we have to develop microgrid solutions to improve people's quality of life, while helping the world be a cleaner, more sustainable place.

Big thank you to my committee members, each of whom has provided me guidance throughout the years and has had great impact on helping shape my academic career at the Swanson School of Engineering. I want to thank Dr. Robert Kerestes for inspiring my thesis topic, knowing I was eager to make my research a humanitarian effort, and for connecting me with David Beeson, who took the time to talk with me about my research and provided insight on Native American traditions and culture and the issues they face today. I also want to thank Dr. Brandon Grainger for providing me mentorship and support throughout the years. To my advisor, Dr. Alexis

Kwasinski, thank you for providing me very helpful and constructive feedback throughout my research. Sincere thanks to my boss, Daniel Carnovale, who was extremely supportive and accommodating of my work schedule during my internship at Eaton's Power Systems Experience Center. A special thanks to Dr. Gregory Reed who was the main reason I pursued a concentration in Power and for providing me with a one-of-a-kind opportunity to continue my studies towards a Master's degree with full scholarship. Thank you all for your unwavering support.

Above all, I would also like to express my sincere gratitude to my parents for their continuous support throughout my academic journey. To my mother, Leyla Nakhai, thank you for providing me with your wisdom and for guiding me throughout the difficult decisions. To my father, Dr. Behnam Nakhai, thank you for inspiring me to continue my education and providing mentorship throughout my academic career. Growing up, you both have encouraged me to be the best student I could possibly be and created an environment for me that made learning feel more rewarding. Thank you for the values you have instilled in me to get me to where I am today.

I could not have done it without the support from you all, the ECE faculty, my cohort in the Power lab, and the support from my friends and family; I'm very grateful and appreciative of you all.

## 1.0 Introduction

Expansion in photovoltaic (PV) cell technology over the past four decades has facilitated a reduction in the capital cost of PV panels, also commonly referred to as solar panels [1]. As a result of reduced costs in the technology, PV powered water pumping has played a critical role in providing water to people living in remote and low-income communities where grid accessibility is hard to maintain and is costly to implement. This technology has played a critical role in improving the quality of life for people living in off-grid rural communities around the world [2]. The benefits of PV water pumping and its success stories among the least developed countries (LDCs) are varied and abundant.

Since the early 1990s, over 10,000 PV water pumping systems have been installed in developing countries like Kenya, Bangladesh, and the Philippines [3]. Case studies from various countries in Africa report the successful implementation and adoption of these systems. In Africa's most populous nation, Nigeria, PV water pumping has become the preferred technology for pumping groundwater with over 760 installations since 2011 and has benefitted about 2 million people [4]. While relatively limited, experience in several countries shows how PV water pumping can increase resiliency against the irregular shifts in rainfall patterns (caused by climate change) or the unreliable supply and high costs of fossil fuels needed to operate water pumps. This technology has the potential to benefit rural populations in a variety of ways, such as agricultural productivity, resilience to climate events and natural disasters, reliable access to clean drinking water, and improvements to health [2].

For the past 30 years, United Nations Children's Emergency Fund (UNICEF) has been among leading international organizations implementing PV powered water supply systems in off-grid communities [4]. In 2016, an assessment performed by UNICEF Solar Powered Water System in 35 communities within four countries (Nigeria, Mauritania, Uganda, Myanmar) concluded that PV powered water systems perform well in terms of flow rate and durability where sunlight is plentiful. The vast majority of pumps were able to provide sufficient water supply throughout the year, the exception being a few days during rain and dry seasons. It was found that this issue could be offset by improving storage capacity or the addition of a back-up generator. These systems were favorable across communities, government, non-governmental organizations (NGOs), and private sector partners and the case studies reflect that PV systems are an alternative to replace conventional fossil fuel-based systems and handpumps.

Solar water pumps were first introduced in sub-Saharan Africa as early as 1970s and only within the last 10-15 years the sharp decline in solar panel prices have gained lots of traction [2]. In fact, with the projected increase in household income and the decrease in the cost of technology over the next decade, the market for solar water pumps in Sub-Saharan Africa is expected to expand to as many as 2.8 million households, totaling to an estimated $1.6 billion in value. Compared to sub-Saharan Africa, implementation of PV water pumping systems for irrigation is higher in India, where over 150,000 solar water pumps are in use today with the help of government subsidies. Within the next few years, India's government has ambitious plans to reach its goal of 1 million solar water pumps in order to help larger farms with high water intensity of crops, such as rice. Estimates show there are currently 4.2 million farming households in India that have demand for solar water pumps and can afford one, versus 700,000 households in sub-Saharan Africa.

There are many examples of successful implementations of PV water pumping systems in rural communities around the world. In 2016 the joint partnership between Water Mission, Nordic

Development Fund, and the World Bank helped fund PV water projects to address the water supply challenges in Northern Tanzania [5]. With the shift to solar, Tanzanian villagers no longer need to walk several miles to retrieve water pumped by diesel generators, which was unsafe to drink and often supplied an unreliable quantity. The implementation of PV water pumping allows communities to pay a fair and sustainable price for water, which is 10 times less than what they were paying before. Aside from financial benefits, the access to clean and safe water has helped communities reduce typhoid cases and fevers from diseases and bacteria. From a techno-economic perspective, these developments speak volumes about the success and the future growth potential of PV water pumping technology, especially in less-developed rural regions where traditional infrastructure is limited or absent.

Lack of access to running water is not only a vital issue among the LDCs, but has also been a pressing issue in the United States. Today, over two million Americans are estimated to be living without access to running water [6]. The vast majority of Native American's, the first citizens of the United States, live in similar sub-standard conditions, as they have been structurally locked out of opportunities that were made available to most other American communities by the mid-twentieth century [7]. In their campaign for westward expansion in the mid-1800s and interest in acquiring Indian land, the United States signed treaties with Native Americans to give up their land and, in exchange, the federal government agreed to guarantee education, health care, housing, and other services to tribes [8]. Many of these promises have gone unfulfilled and the broken treaties have made the life of Native American tribes a struggle. Native Americans consider water to be a sacred element and the source of all life, as they believe it ensures physical and psychological well-being [9]. Most Native American reservations throughout the country are left without adequate access to basic needs, such as clean water, plumbing, electricity, roads, housing, and public transportation, let alone hospitals, schools, internet, and cellular services. In fact, it is estimated that 13.3% of Native Americans lack accessibility to safe drinking water today, which indicates that the federal government's support for Native American economic and infrastructure development continues to be grossly inadequate. Funding remains far below the threshold needed to remove the barriers for any viable economic development program for Native American tribes. The Navajo Nation is just one among hundreds of reservations in the U.S. wishing to implement solutions to meet the most basic needs the federal government is obligated to provide. Since the cost of transmission extension is not economically viable, there are valuable lessons to be learned and emulated from the successful PV water pumping projects in LDCs that can be applied to off-grid Native American reservations in the U.S.

In this study, a PV-battery water pumping system is proposed. Although they are more affordable than grid extension, they can be expensive to maintain. For this reason, this study takes a close look at the effects climate change can have on the economics of a PV-battery microgrid system for rural off-grid communities located in hot climates. This study highlights the importance of considering environmental and operating temperature conditions for power system design and their effects on life, sizing, and the economics of a system.

The remainder of this thesis is organized as follows. Section 2 discusses PV-battery water pumping technology and its technical design requirements. This is followed by Section 3 in which the case of the Navajo Nation's water crisis is explored. Section 4 focuses on system layout and sizing and provides quantitative and simulation results from HOMER Pro. The economic analysis of the results is performed and discussed in Section 5. Finally, a discussion of the findings, implications, and suggestions for future work are presented in Section 6.

## 2.0 PV-Battery Water Pumping

Traditionally, water pumps extract water from surface or underground water resources using conventional electricity or diesel generation as the power source [2]. Throughout the past few decades, expansion in PV technology has resulted in reduced costs of PV panels. Since the 1970s, the price of PV panels has decreases significantly, from about $76 per Watt to about $0.3 per Watt. As a result, PV water pumping has become an economically viable and common solution for water in low-income rural communities across the world with minimal or no access to power [8]. The significant decrease in PV panel costs combined with the increase in pump manufacturers has facilitated an 80% decrease in the cost of PV water pumping systems over the past two decades [2]. In addition, early solar pumps had limited performance and could only reach wells less than 200 meters deep and could on benefit applications with water demand less than 300 $m^3$/day [10]. Today, solar pumps can reach deeper wells (about 500 meters) and push larger volumes of water at about 1,500 $m^3$/day. Efficiencies of solar pump technologies have also increased considerably.

### 2.1 Technology & Operation

A PV-battery water pumping system can be used to pump water with very few main components and without any distribution networks [11]. The key system components are as follows:

1. **PV array**, which is the DC power source for the system and for charging the batteries [12]. The PV array must be sized correctly to meet the pump motor and load requirements.

2. **Charge controller/regulator**, which is used to regulate the voltage between the PV array and the batteries in order to protect the batteries from overcharging and potential damage [12].
3. **Converter or inverter,** which is used to convert the DC power generated by the PV array, depending on if the system is classified as a DC or AC motor-based system [2].
4. **AC or DC Motor,** which drives the water pump by converting the electrical energy produced by the PV array to mechanical energy [10].
5. **Water pump**, which physically lifts the water from the source to the point of use or storage and is an essential part of the system design in order to meet the water demand requirements [10].
6. **Water storage and batteries**, which can be used to ensure continuous supply of water [12]. Batteries can be used to store excess power generated by the PV array to provide continuous flow of electricity in the event that there is little to no solar radiation, like during a cloudy period or nighttime hours.

## 2.2 System Parameters

Since solar pumps cannot deliver water on demand, a careful assessment of the solar potential and accurate measure of water demand is required [11]. The design of PV water pumping systems is best accomplished by analyzing the following key system parameters:

1. **Water Demand:** The design capacity of a solar water pumping systems depends primarily on daily water output ($Q$), which is measured in $m^3$/day [10]. The water demand is estimated from the population size and the daily water consumption per capita. This parameter can be calculated as follows:

$$Q = (population) \times (per\ capita\ consumption) \tag{2-1}$$

2. **Water Storage:** In general, a system's total water storage capacity should be sized to store enough water for at least 3 days of water supply [10]. The minimum storage volume ($V_{tank}$) can be sized as follows:

$$V_{tank} = Q \times 3\ days \tag{2-2}$$

3. **Solar Data:** *Solar irradiance* ($G$) is the amount of solar radiation onto earth's surface per unit area, commonly expressed in units of kWh/m$^2$/day [10]. Irradiance is affected by the angle of the sun and changes throughout the day as the sun's position changes. As shown in Figure 1, solar irradiance increases during the morning until noon where it reaches the peak and is highest when the incident sun rays are perpendicular to the PV module, then decreases until sunset. *Solar insolation* ($I$) is the amount of solar irradiance measured over a given period of time and is shown in Figure 1 as the area under the solar irradiance curve. It is typically quantified in peak sun hours and is also expressed in units of kWh/m$^2$/day.

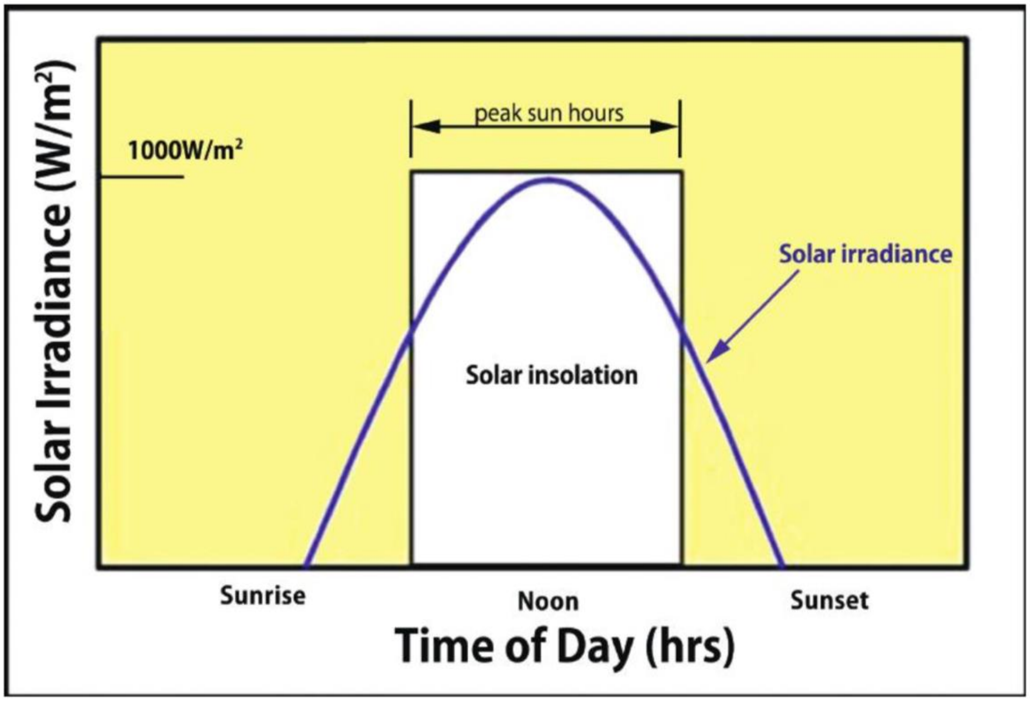


**Figure 1 Solar Irradiance vs. Time of Day**

4. **Total Dynamic Head:** In pumping systems, the total dynamic head ($TDH$) refers to the total height that the pump must overcome in order to deliver the required amount of water, as illustrated in Figure 2 [2]. The TDH is a sum of three components, including the static head, discharge head, and friction head [10]. Static head is the actual vertical distance measured from the minimum water level to the highest point in the discharge piping. Discharge head corresponds to the height from the ground of the water surface to the storage tank. The TDH can be calculated as follows:

$$TDH = Static\ Head + Discharge\ Head + Friction\ Head \tag{2-3}$$

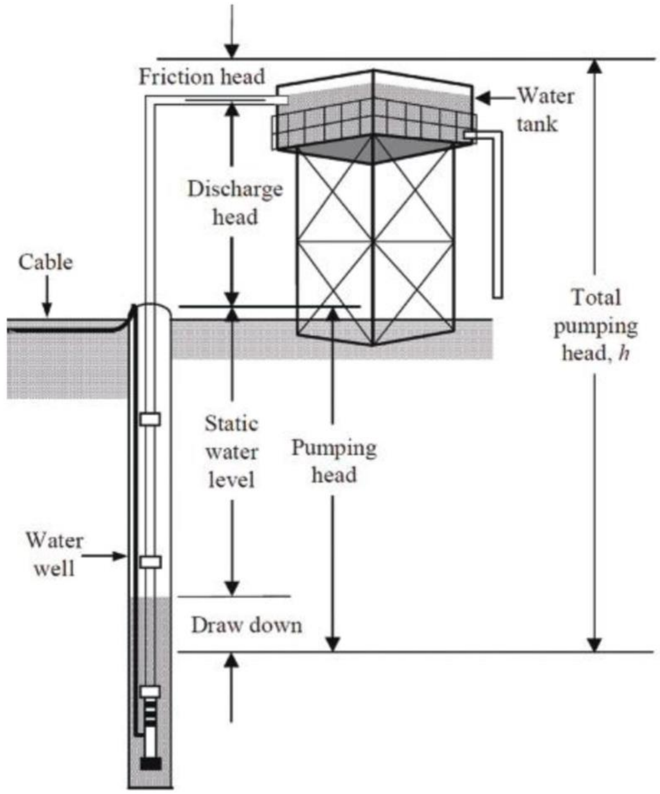


**Figure 2 Total Dynamic Head Determination for a Water Well**

5. **Energy Requirement:** The *hydraulic energy* ($E_h$) requirement is the potential energy required in raising the water to the discharge level and is measured in kWh/day [10]. The *electrical energy* ($E_E$) requirement is the kWh/day value needed to meet the load demand. By knowing the daily water output ($Q$), density of water ($\rho$), total dynamic head ($TDH$), acceleration due to gravity ($g$), and motor-pump efficiency ($\eta_M$), the energy requirements can be determined as follows:

$$E_h = \frac{Q \times TDH \times \rho \times g}{3{,}600{,}000} \tag{2-4}$$

$$E_E = \frac{E_h}{\eta_M} \tag{2-5}$$

6. **PV Array Capacity:** By utilizing the data for solar irradiance ($G$), efficiency ($\eta_{PV}$) and area ($A_{PV}$) of the selected PV panel, the electrical energy requirement ($E_E$), and the maximum power output of the panels ($W_{p,PV}$), the required number of PV panels ($N_{PV}$) and the required power output of the PV array ($P_{PV}$) can be determined, as follows:

$$N_{PV} = \frac{E_E}{G \times \eta_{PV} \times A_{PV}} \tag{2-6}$$

$$P_{PV} = N_{PV} \times W_{p,PV} \tag{2-7}$$

## 3.0 The Case of the Navajo Nation

The Navajo Indian Reservation, founded in 1868, is the largest federally-recognized sovereign Native American reservation in the United States with a population over 170,000 people [13]. It is split into five agencies, as shown in Figure 3. Each agency is geographically and politically divided into a total of 110 different chapters across all agencies. These chapters serve as sub-governmental entities to address local issues pertaining to the land and health status of their respective chapter population [14].

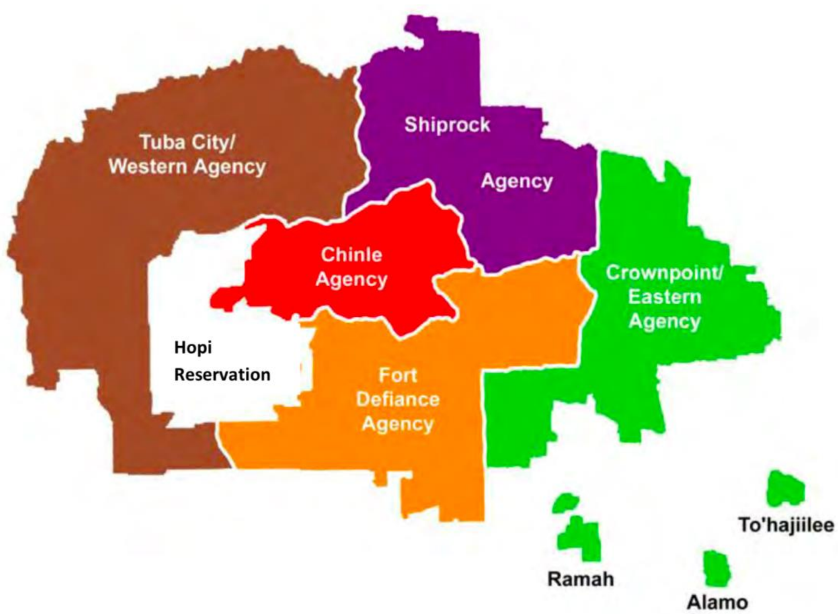


**Figure 3 Map of the Five Agencies on the Navajo Nation**

The reservation extends across three states in the Southwest, including: Arizona, Utah, and New Mexico and covers over 27,000 square miles of arid deserts and alpine forests with high plateaus, mesas, and mountains [15]. Since the Navajo Nation is located in an isolated and rural area, the cost of power line extension is very costly, making it economically infeasible for most homeowners to acquire centralized water systems, especially when considering their economic condition and the limited government funding [16]. These challenges have hindered progress towards implementing water infrastructure in the Navajo Nation. Today, most Navajo residents live without access to basic needs, such as running water, reliable lighting, modern forms of home heating and cooling, and appliances such as refrigerators.

## 3.1 Water Accessibility

The Navajo Department of Water Resources reports that approximately 30% of the population does not have direct access to running water in their homes, and every few days must haul water, sometimes as far as 40 miles, for drinking, cooking, and bathing [17]. The severity of the problem can be understood best if one considers the following disparity in the standard of living between Navajo residents and the average American: Many Navajo residents have less than 10 gallons of water at home at any given time, use as little as 2-3 gallons of water per day, and pay an average of $0.13 for a gallon of water [13]. In comparison, the average American, who has access to endless running water, uses about 88 gallons of water per day, and the typical suburban Arizona resident pays 72 times less for a gallon of water. For a population that is among the poorest in the U.S., water is among the most expensive. Given the limited tribal resources and the limited federal budgets and authorizations, the water resource problems will become increasingly acute, intensifying the poor socioeconomic conditions on the Navajo reservation [18]. The Indian Health Service, an agency within the Department of Health and Human Services, estimates over $200 million worth of infrastructure would be needed to provide all Navajo homes access to safe drinking water and basic sanitation [17].

The LeChee Chapter is one of the only chapters in the Western Agency without any groundwater wells and the proposed system in this study is designed and sized for this community. Due to its lack of water access points, the LeChee Public Water System serves the water demand of its community by purchasing potable water from the City of Page, located about 4 miles away [19]. This water is supplied from Lake Powell, the largest reservoir in the Colorado River system, and about 100,000 gallons of treated water is delivered to the LeChee community per day [20].

## 3.2 Water Availability & Climate Change

Climate change is a relevant issue affecting the reliability of water on the Navajo Nation and it is important to understand and evaluate how these changes will further impact the availability of fresh water when planning for solutions [21]. With the rapidly changing climate, especially in the Southwest region, streamflow and surface water resources, like Lake Powell, are at increased risk. As shown in Figure 4, Arizona's temperature projections are expected to rise significantly in the upcoming decades [22]. An increase in air temperature is projected to intensify naturally occurring droughts and, as a result, surface water is expected to experience reduced flows and gradual depletion. Long-term droughts will not only further challenge limited water resources, but also increase the frequency and severity of wildfires, which is already a concern for this arid state.

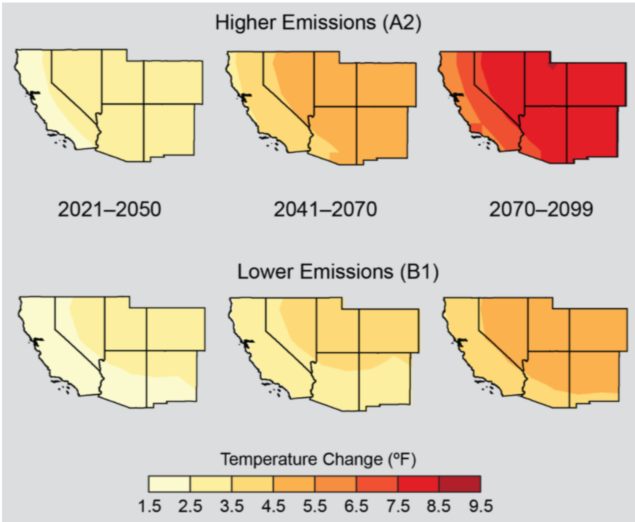


**Figure 4 Projected Changes in Average Annual Temperatures in Southwest U.S.**

Rain and snowfall are key elements to Earth's water resources, as rain and melted snowfall are typically plentiful in the spring and summers. However, over the past century, the Navajo Nation has experienced long-term decreases in annual rain and snowfall [23]. As shown in Figure 5, spring precipitation in northern Arizona is projected to decrease 5% to 10% by the mid-twenty first century [22].

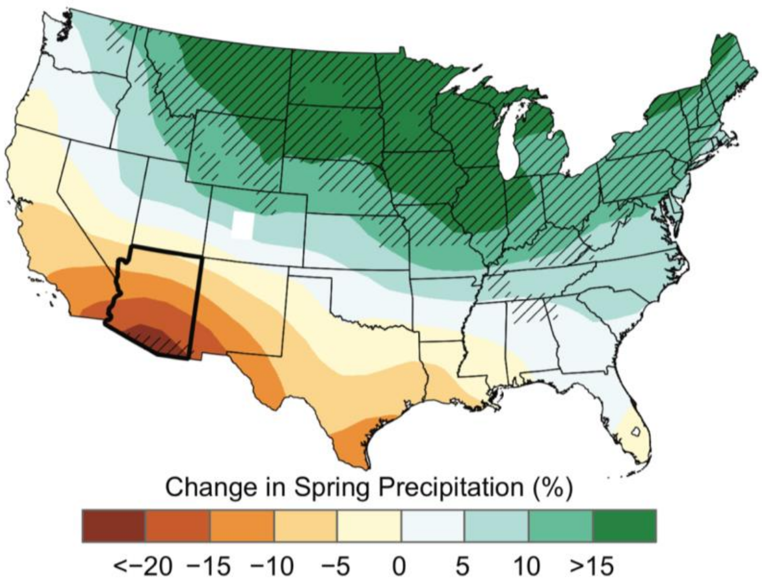


**Figure 5 Projected Changes in Spring Precipitation by Mid-21st Century**

As a result, this is projected to further reduce late season snowpack accumulation in the mountains and decrease flows in the Colorado River and water supply in reservoirs, like Lake Powell [22]. This reduction in water flow can severely affect communities, like LeChee, that rely on the snowpack for summer water supplies. The projected rise in spring temperatures will also result in earlier melting of the snowpack, further decreasing water resources needed during the summer. According to the National Oceanic and Atmospheric Administration (NOAA), there is a 50% chance of full depletion of the Colorado River reservoir storage by mid-twenty first century [24]. The limited resources and poor economic conditions constrain the Navajo Nation's ability to respond effectively to these changes.

Fortunately, there are adequate groundwater aquifers available that can serve communities on the Navajo Nation, as shown in Figure 6 [19]. Although the C-Aquifer is dry across the LeChee chapter, the Navajo (N) Aquifer provides opportunities for implementing water pumping from groundwater resources. According to the National Institute of Science, the N-Aquifer is one of the most "pristine" water sources and is among the few sources of drinking water in the U.S. that naturally meets the Environmental Protection Agency's standard for drinking water. In fact, it is one of northeastern Arizona's most productive aquifers for dependable water supply.

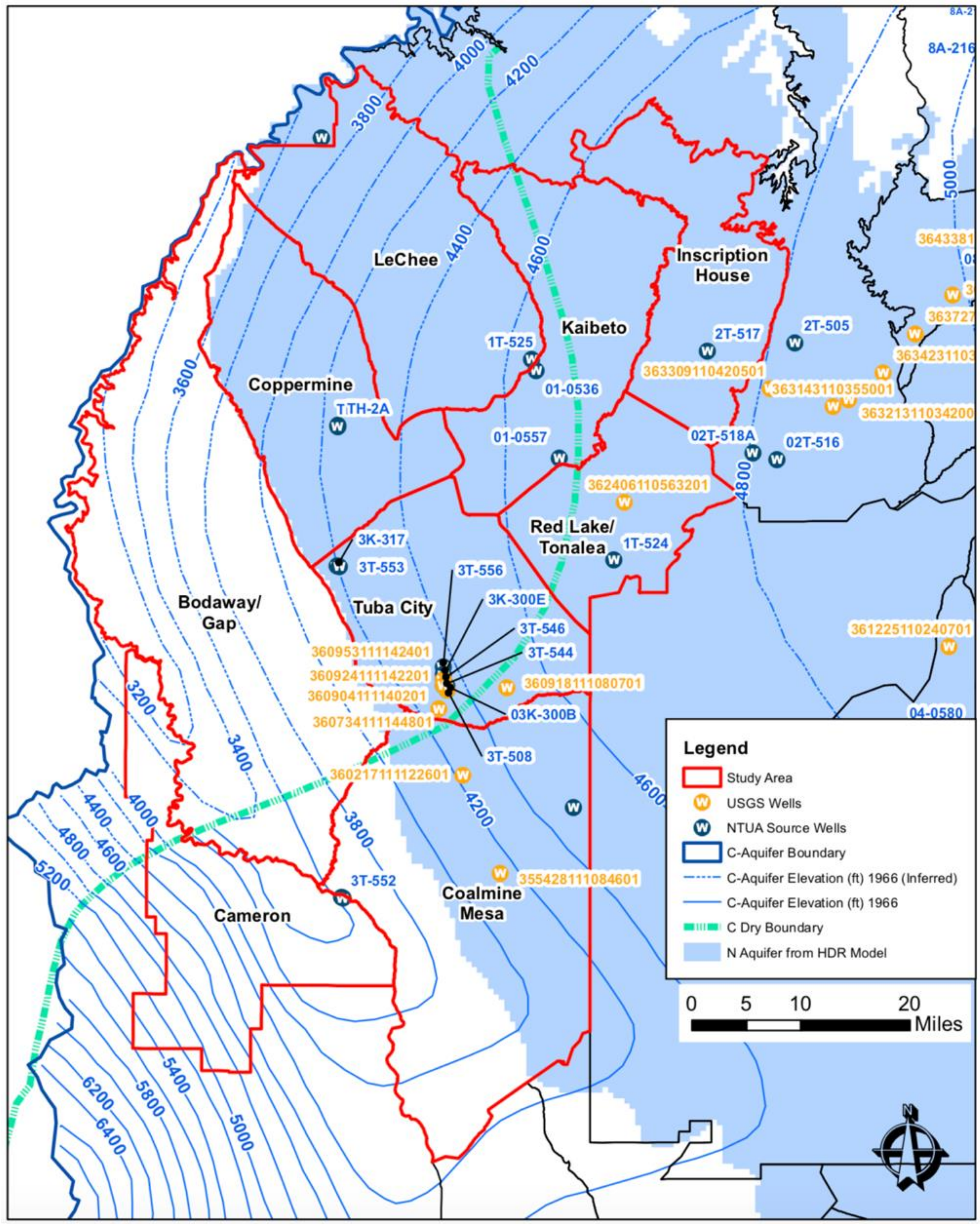


**Figure 6 Groundwater Aquifers in Navajo Nation's Western Agency**

## 4.0 System Design & Sizing

Electric water pumping systems can be classified as either DC or AC systems, depending on the type of motor used [2]. Since PV panels convert light energy into DC power, the power can be directly supplied to a DC motor or it can be converted to AC using an inverter to drive an AC motor. Figure 7 shows four possible ways of power transfer from PV to either DC or AC motor applications and are described as follows:

1. PV driven AC motor with inverter (line 1)
2. Direct PV driven DC motor (line 2)
3. PV driven AC motor with DC-DC converter and inverter (line 3)
4. PV driven DC motor with DC-DC converter (line 4)

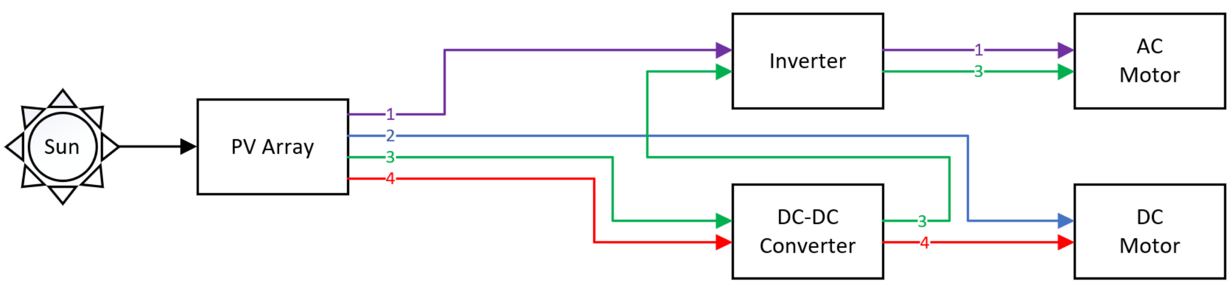


**Figure 7 Classification of PV Driven Motors**

For this study, a PV driven DC motor with a DC-DC converter is considered. DC systems have become lauded for their potential to reduce power conversion losses, improve power quality, and reduce costs of power systems [25]. DC motors have been widely used for speed or position control applications because of their simple speed/torque control and excellent drive performance. However, AC motors have been preferred for most motor drive applications since DC motors require mechanical commutation devices, consisting of brushes and commutators, that change the direction of the current of conductors to produce an average torque for continuous rotation. Since these mechanical parts require periodic maintenance, AC motors have been preferred in motor drive applications that demand long life and reliability, as traditional DC motors are less reliable and unsuitable for a maintenance-free operation. To overcome this challenge, the brushless DC (BLDC) motor was developed in 1962, which has similar electrical characteristics to the traditional DC motor, but the mechanical commutation is replaced with sensors and driving circuits for electronic commutation.

BLDC motors have a different configuration from that of traditional DC motors because the armature windings are placed on the stator side and permanent magnets are placed on the rotor side [25]. The sensors detect the position of permanent magnets on the rotor and based on this information the driving circuits decide which winding to energize for continuous rotation. Compared to induction motors, BLDC motors consume less power because they do not require current to be induced in rotor windings and the elimination of brushes contributes to increased efficiency, reliability, and durability [2]. This makes these motors ideal for use in applications with varied loads, such as PV water pumping, because they have integrated controls or are paired with drives. For this study, a BLDC motor is not only a cost-effective solution, but it has many merits such as high efficiency, high-power density, high torque-to-inertia ratio, high-speed operation capability, and simple drive method [25]. The system layout for the proposed PV-battery water pumping system is shown as a block diagram in Figure 8.

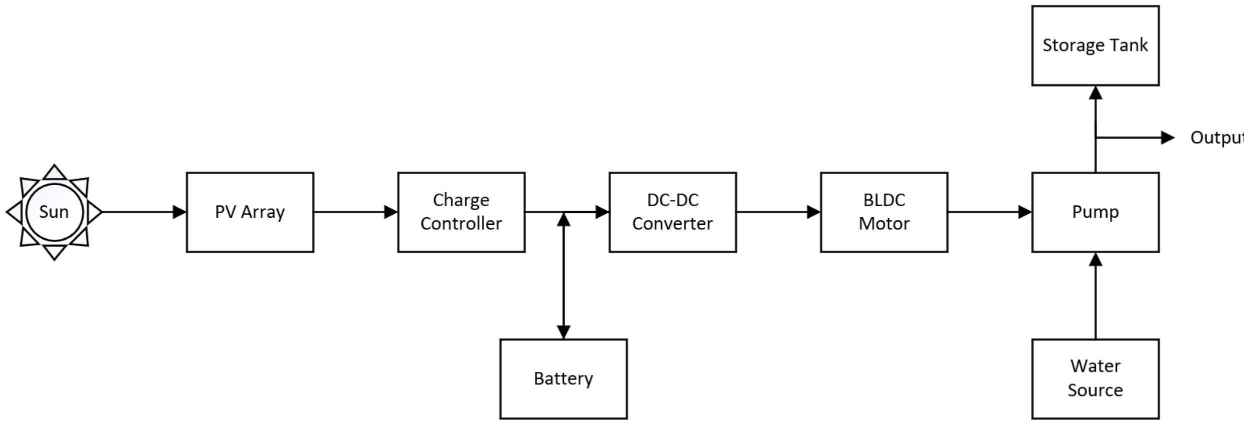


**Figure 8 Block Diagram of Proposed PV-Battery Water Pumping System**

The performance of the motor depends on the input voltage from the PV array. This can be seen by the DC motor voltage equation:

$$V = E + I \cdot R + V_b \tag{4-1}$$

where $V$ is the applied voltage, $E$ is the motor back e.m.f., $I$ is the armature current, $R$ is the armature resistance, and $V_b$ is the brushes voltage drop [26]. The rotor speed and flow rate from the pump are proportional to solar irradiation, which varies each day depending on the weather conditions. In the event that there is little or no sunshine, the batteries provide the power and, when discharging, the voltage at the output of the batteries and input to the motor will drop. Thus, a DC-DC converter between the battery and motor will regulate the input voltage to the motor and will allow the motor to run at constant speed, even at different solar irradiation levels, in order to maintain a consistent flow rate of water. This can improve the efficiency of the water pump, which is dependent on the input power.

## 4.1 Battery Storage

Most rural areas in the United States have already experienced the impacts of climate change and observed warming trends are expected to increase in the coming decades [27]. This presents a new challenge for battery supported systems, as consistent operation outside of temperature ranges recommended by the original equipment manufacturer (OEM) can significantly affect the performance of batteries and lead to faster degradation. The relationship between battery state of health (SOH) and charging cycles is depicted in Figure 9.

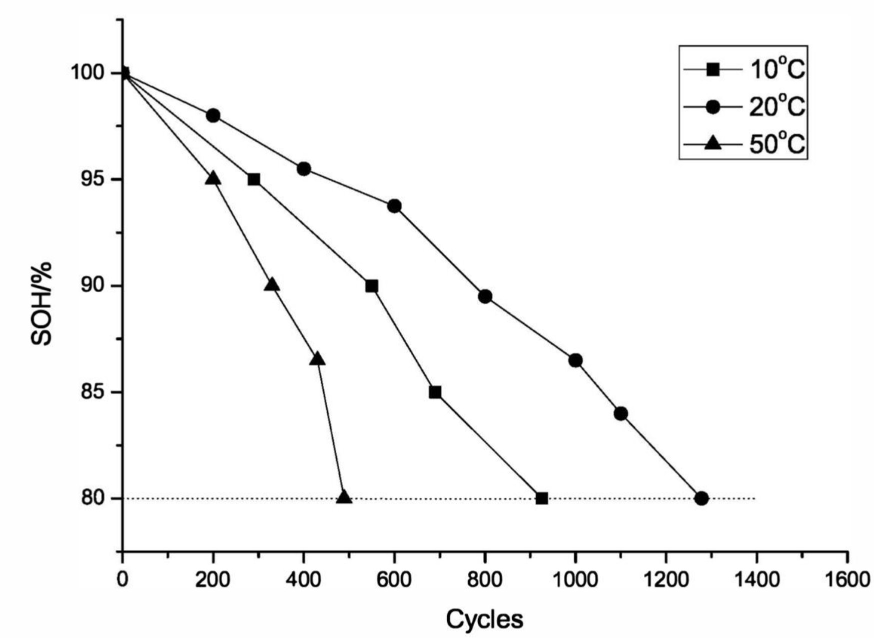


**Figure 9 Battery SOH and Charging Cycles at Different Temperatures**

As a battery degrades, the effective capacity of the battery to store and discharge energy decreases over time [27]. The state of charge (SOC) of a battery refers to its level of charge relative to its capacity and varies between 0% and 100%. Overtime, as a battery degrades, its maximum SOC starts decreasing [28]. Typically, a battery is assumed to be at the end of its useable life when it can only store 80% of its original available capacity. Batteries account for a significant portion of capital costs during the life of a system, making understanding the relationship between temperature and expected lifetime in warmer climates critical in system design and ultimately important in understanding overall economics of the project. There are a number of factors that can affect the lifetime of batteries. For the purpose of this study, only the direct effects that variations in air temperature has on the internal chemical reactions of the battery cell are considered.

The Arrhenius equation shown below models the temperature dependence of certain chemical reactions and is a common approach to understand the effect of temperature on battery degradation:

$$K = Ae^{\frac{-E_a}{RT}} \tag{4-2}$$

where $K$ is the rate constant, $A$ is the frequency factor, $E_a$ is the activation energy representing the energy barrier for the chemical reaction, $R$ is the universal gas constant (or Boltzmann's constant), and $T$ is the absolute temperature in Kelvin [29]. Internal chemical reactions in a battery are driven by voltage and temperature [30]. As battery temperature increases, the rate of chemical reactions increases and results in a corresponding loss of battery life. An off-shoot Arrhenius equation is the "decade rule", which states that the useful life of the battery doubles for every 10°C decrease in temperature, or that the aging rate doubles for every 10°C increase.

This study attempts to quantify the effects climate change can have on the lifetime of lead acid batteries at a minimum SOC (MSOC) level of 50%, which is commonly used in practice [31]. Given the uncertainties inherent in projecting the magnitude of future temperature increases due to climate change, estimating the lifetime of batteries can be quite difficult. In light of these uncertainties, the “three-point estimation” [32] technique is applied in this research, which is a technique used in decision sciences to estimate the output of future events based on limited information. The three scenarios are defined as follows:

1. **Optimistic estimate (*O*):** The minimum temperature increase, if climate change occurs ideally low and manageable.
2. **Most likely estimate (*M*):** The most probable temperature increase, if climate change patterns occur as projected.
3. **Pessimistic estimate (*P*):** The maximum temperature increase, if climate change impacts are substantial.

The considered optimistic, most likely, and pessimistic temperature increases by 2050 (projected by the NOAA) are shown in Table 1 [22].

**Table 1 Projected Temperature Increases by 2050**

| Scenario | Temp. Increase |
|---|---|
| Optimistic (*O*) | 2°F |
| Most Likely (*M*) | 4°F |
| Pessimistic (*P*) | 6°F |

## 4.2 System Sizing

According to the U.S. Census Bureau, LeChee has a population of about 1,660 residents [33]. The water consumption per capita in LeChee is about 45 gallons per day, compared to a national average of about 85 gallons per day [20]. This study aims to provide an adequate number of water access points with the proposed PV-battery operated water pumping system to minimize long distance traveling and water hauling. In doing so, the goal is to achieve a standard of living that can accompany an increase in water demand and meet the future water needs of the LeChee community.

### 4.2.1 Technical & Economic Assumptions

Given the LeChee community's size, geography, and underground water sources, this study considers ten PV-battery water pumping systems for every 166 people. The system is sized to meet a projected per capita water demand of 55 gallons per day for a 25-year time period. A 5% discount rate is assumed and the Federal Reserve's target inflation rate of 2% will be applied for cost analysis purposes [34]. Table 2 summarizes the assumptions used for the proposed system.

**Table 2 Assumptions for Proposed System**

| **Parameter** | **Value** |
|---|---|
| Population per system | 166 people |
| Number of Systems | 10 |
| Per Capita Water Consumption | 55 gallons/day |
| Discounting Rate | 5% |
| Inflation Rate | 2% |
| System Lifetime | 25 years |

For this study, generic flat plate 1 kW PV panels are considered. Each panel is assumed to have an area of 1.7 $m^2$ and module efficiency is assumed to be 13%. To maximize overall production year-round, the tilt of the PV array is set to the latitude of the location, which is 37° for LeChee, AZ [35]. The azimuth, or the horizontal orientation of the panels in relation the Equator, produces best results when the panels face toward the Equator [35]. Therefore, the azimuth is selected to be 180°. According to a study conducted by the National Renewable Energy Laboratory

(NREL) in 2017, the cost of utility-scale fixed-tilt PV is approximately $1.11/W [36]. The lifetime of the panels is assumed to be 25 years, with estimated annual operation and maintenance (O&M) cost of $10/kW. The assumptions used for the PV panels are further detailed in Table 3.

**Table 3 Assumptions for PV Panels**

| Parameter | Value |
| --- | --- |
| Capital Cost | $1.11/W |
| Rated Capacity | 1 kW |
| Panel Area | 1.7 $m^2$ |
| Module Efficiency | 13% |
| Operating Temp. | 47°C |
| Maintenance Cost | $10/kW/year |
| Derating Factor | 80% |
| Tilt | 37° |
| Azimuth | 180° |
| Panel Lifespan | 25 years |

For this study, a lead acid battery is considered as the storage component. The selected battery model is Trojan SIND 06 1225, which has 6 V nominal voltage and 7.69 kWh of energy storage capacity [30]. This study is based on a 50% MSOC, as noted previously. The cost of capital with installation included is $2,205 per battery with estimated O&M cost of $10/year. The life of the battery, according to the OEM, is 17 years when it is operated consistently at 25°C [30]. Table 4 outlines the assumptions used for the battery in the proposed system.

**Table 4 Assumptions for Battery Storage**

| **Parameter** | **Value** |
|---|---|
| Battery Model | Trojan SIND 06 1225 Lead Acid |
| Capital Cost | $2,205 |
| O&M Cost | $10/year |
| Nominal Voltage | 6 V |
| Energy Rating | 7.69 kWh |
| Capacity | 1225 Ah |
| Mass | 188 kg |
| Maximum Operating Temp. | 45°C |
| Minimum Operating Temp | -20°C |
| Minimum State of Charge (MSOC) | 50% |
| Lifetime | 17 years |
| Degradation Limit | 20% |

As for the proposed system's operation, it is assumed that it will operate for 19 hours a day (4:00 AM to 11:00 PM), as shown in the daily load profile in Figure 10. Within this time frame, the system is assumed to operate for 10 minutes every hour resulting in a total daily operation time of 190 minutes and a total operation time of 28,896 hours in the 25-year lifetime of the system. Table 5 summarizes the assumptions made for the system's operation used for this study. The peak demand is assumed to occur between 7:00 AM – 11:00 AM and between 4:00 PM – 8:00 PM with a peak load of about 2.87 kW.

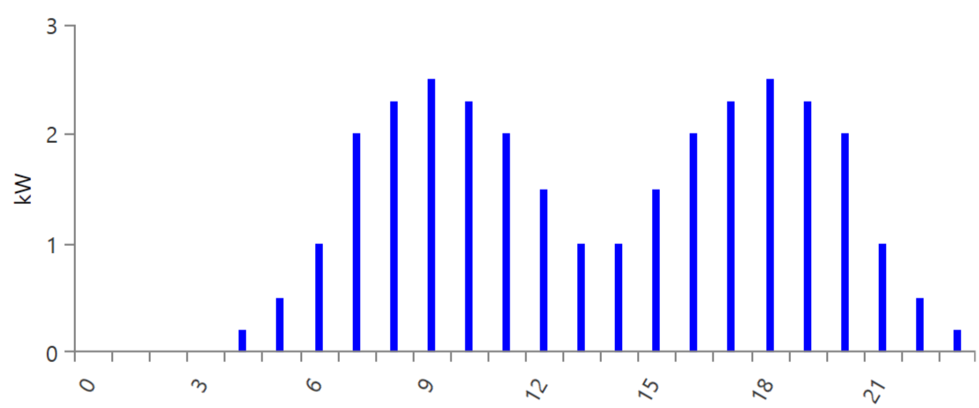


**Figure 10 Daily Load Profile**

**Table 5 Assumptions for System Operation**

| System Operation | Time |
|---|---|
| Daily Length of Operation | 19 hours |
| Operating Increments | 10 minutes/hour |
| Daily Operation | 190 minutes |
| Lifetime Operation (25 years) | 28,896 hours |

### 4.2.2 Quantitative Results

Properly sizing the proposed PV-battery microgrid system involves determining the electrical energy requirement, which is needed to calculate the required power output of the PV array ($P_{PV}$) and battery storage capacity ($E_B$). The first step is to determine the required daily water output ($Q$) for the system. Using the projected per capita water demand of 55 gallons/day and population of 166 people per system, $Q$ is determined to be:

$$\begin{aligned} Q &= (population) \times (per\ capita\ demand) = 166\ people \times 55\ \frac{gallons}{day} \\ &= 9{,}130\ \frac{gallons}{day}\ or\ 35\frac{m^3}{day} \end{aligned} \tag{4-3}$$

The second step is to determine the required water storage volume ($V_{tank}$). The system's water tank is sized to store an adequate amount of water for at least 3 days of basic water needs. Thus, the water tank should be able to store a minimum of:

$$V_{tank} = Q \times 3\ days = 9{,}130\ \frac{gallons}{day} \times 3\ days = 27{,}390\ gallons\ or\ 104\ m^3 \tag{4-4}$$

Next, the pumping hydraulic energy requirement ($E_h$) needs be determined. To calculate this value, the TDH is assumed to be 130 m, density of water ($\rho$) is 1,000 kg/m$^3$, and gravity ($g$) is 9.8 m/s$^2$. Thus, the hydraulic energy required to supply the water flow rate, $Q$, can be calculated as:

$$E_h = \frac{Q \times TDH \times \rho \times g}{3{,}600{,}000} = \frac{35\ \frac{m^3}{day} \times 130\ m \times 1000\ \frac{kg}{m^3} \times 9.8\ \frac{m}{s^2}}{3{,}600{,}000\ \frac{J}{kWh}} = 12.23\ \frac{kWh}{day} \tag{4-5}$$

Now, the electrical energy requirement ($E_E$) can be determined. Assuming motor-pump efficiency ($\eta_M$) of 60%, the effective electrical energy requirement for the proposed system will be:

$$E_E = \frac{E_h}{\eta_M} = \frac{12.23\ \frac{kWh}{day}}{0.60} = 20.38\ \frac{kWh}{day} \tag{4-6}$$

Next, based on NREL's global horizontal irradiance data from [37], the average solar irradiance ($G$) on the Navajo Nation is 5.04 kWh/m$^2$/day and using the assumed PV panel efficiency ($\eta_{PV}$) of 13%, the usable solar irradiance ($G_{eff}$) per day will be:

$$G_{eff} = G \times \eta_{PV} = 5.04\ \frac{\frac{kWh}{m^2}}{day} \times 0.13 = 0.6552\ \frac{\frac{kWh}{m^2}}{day} \tag{4-7}$$

Using this value and the assumed PV panel area ($A_{PV}$) of 1.7 m$^2$, the energy consumption per panel ($E_{PV}$) is calculated as:

$$E_{PV} = G_{eff} \times A_{PV} = 0.6552 \ \frac{\frac{kWh}{m^2}}{day} \times 1.7\, m^2 = 1.1138 \ \frac{kWh}{day} \tag{4-8}$$

With this information, the required number of PV panels ($N_{PV}$) will be:

$$N_{PV} = \frac{E_E}{E_{PV}} = \frac{20.38 \ \frac{kWh}{day}}{1.1138 \ \frac{kWh}{day}} = 18.3\, panels \tag{4-9}$$

Finally, with the assumed PV panel rating ($W_{p,PV}$) of 1 kW, the required power output of the PV array ($P_{PV}$) will be:

$$P_{PV} = N_{PV} \times W_{p,PV} = 18.3\, panels \times \ 1 \ \frac{kW}{panel} \ = 18.3\, kW \tag{4-10}$$

Given the Navajo Nation experiences annual solar radiation ($I$), or peak sun hours ($t_I$), of 6.57 kWh/m$^2$/day (see Appendix A) and the system's operation time span ($t_{op}$) of 19 hours/day, the required battery storage capacity ($E_B$) can be calculated as follows:

$$E_B = \frac{E_E}{24 \ \frac{hr}{day}} \left(t_{op} - t_I\right) = \frac{20.38 \ \frac{kWh}{day}}{24 \ \frac{hr}{day}} \left(19 \frac{hrs}{day} - 6.57 \frac{hrs}{day}\right) = 10.6\, kWh \tag{4-11}$$

In an ideal setting, sizing the battery storage bank for a system is not a complex task. For example, the battery storage demand ($E_B$) of 10.6 kWh/day requires a 10.6 kWh battery capacity.

However, the Trojan SIND 06 1225 battery used for the proposed system has a nominal capacity ($E_{B,nominal}$) of 7.69 kWh, which results in a requirement of 2 battery units. Assuming 2 days of autonomy ($t_A$), then 4 battery units will be required. Further, assuming 50% minimum SOC, then the total number of batteries ($N_B$) required for the system would be 8 units, as shown in Equation 4-12.

$$N_B = \frac{\left(\frac{E_B}{E_{B,nominal}} \cdot t_A\right)}{1 - SOC} = \frac{\left(\frac{10.6\ kWh}{7.69\ kWh} \cdot 2\ days\right)}{1 - 0.5} = \frac{(2 \cdot 2)}{0.5} = 8\ batteries \qquad (4\text{-}12)$$

However, in realistic settings this estimation can become insufficient to meet system loads when considering battery life degradation under extreme air temperatures [38]. The number of required batteries is further analyzed in the next section, where effects of temperature variations based on the optimistic, most likely, and pessimistic scenarios are evaluated and compared with and without temperature effects. A summary of the quantitative results for system sizing is shown in Table 6.

**Table 6 Summary of Quantitative Results for System Sizing**

| **Parameter** | **Value** |
|---|---|
| Daily Water Output ($Q$) | 9,130 gallons/day |
| Water Tank Volume ($V_{tank}$) | 27,390 gallons |
| Hydraulic Energy Requirement ($E_h$) | 12.23 kWh |
| Electrical Energy Requirement ($E_E$) | 20.38 kWh/day |
| PV Capacity ($P_{PV}$) | 18.3 kW |
| Number of Batteries Required ($N_B$) | 8 units |

### 4.2.3 HOMER Pro Simulation

In order to support the quantitative sizing results, the HOMER Pro software is utilized for this study. HOMER Pro is a techno-economic modeling software developed by NREL and is a useful tool in optimizing microgrid design based on the net current costs of utilities and sensitivity analysis on uncertain variables [39]. The sensitivity, or “what-if”, analysis tool allows the user to explore the influence of changing an item or variable on the whole system. By performing a sensitivity analysis and specifying a range of values for each component, the software generates results which allow for determining how “sensitive” the outputs are to changes in a specific variable. In HOMER, the best possible, or optimal, system configuration is the one that satisfies the load demand at the lowest Net Present Cost (NPC), which is used to represent the life-cycle cost of the system. To calculate NPC, HOMER uses the following equation:

$$C_{NPC} = \frac{C_{ann,tot}}{CRF\left(i, R_{proj}\right)} \tag{4-13}$$

where $C_{ann,tot}$ is the total annualized cost, $i$ is the discount rate, $R_{proj}$ is the project lifetime, and *CRF* is the capital recovery factor [35].

#### 4.2.3.1 Simulation Inputs

The input data required for the HOMER simulation includes annual load profile, average monthly temperatures, and technical and economic data of system components. HOMER offers the optimized structures and component dimensions that can supply the load and performs an hourly simulation of all possible combinations of components and sizing for analysis. Figure 11 shows the considered generation sources (PV and lead acid battery storage) for the proposed off-grid microgrid system to meet the load demand of the LeChee community.

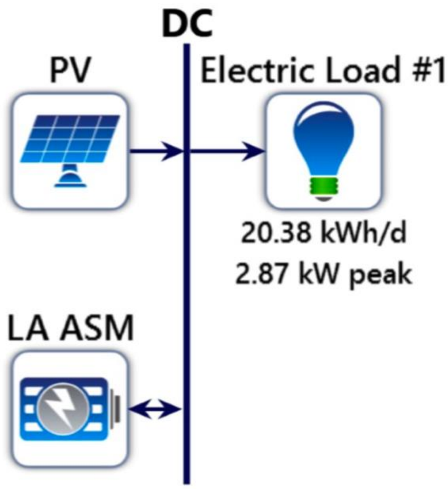


**Figure 11 HOMER Schematic of Proposed System**

As discussed earlier, the effect of air temperature on the battery storage component is considered in this analysis. In order to model temperature effects on battery performance and lifetime, HOMER offers a "Modified Kinetic Battery Model" feature, which adds a series resistance ($R_0$) to model temperature effects on capacity, degradation rate, and cycle-by-cycle degradation based on depth of discharge (DOD) [39]. The functional model is shown in Figure 12.

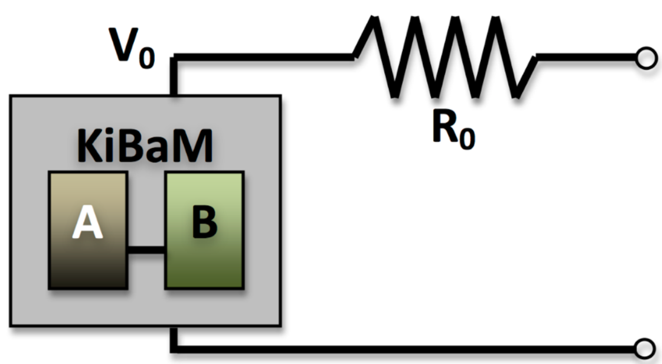


**Figure 12 HOMER Functional Model of Modified Kinetic Battery**

Any energy dissipated by the effective series resistance is converted to heat, which increases the bulk temperature of the storage bank. Based on the monthly ambient temperatures, which are manually inputted based on the optimistic, most likely, and pessimistic scenarios, heat dissipates to or is absorbed from the air temperature of the environment which the system is located. Losses in the series resistance that are converted to heat is given by:

$$\dot{Q} = I^2 R_0 \tag{4-14}$$

where $I$ is the current in amps, and $R_0$ is the series resistance in ohms [39]. This heat generation and rate of heat exchange drives a rate of change in the battery's internal temperature. This energy balance is given by:

$$mc\dot{T} = \dot{Q} - (T - T_a)h \tag{4-15}$$

where $m$ is the mass of the battery in kg, $c$ is the specific heat capacity in J/kgK, $h$ is the thermal conductance to ambient, $\dot{T}$ is the rage of change in K/s, $T$ is the internal temperature of the battery, and $T_a$ is the ambient temperature in K [39]. HOMER uses the solution to this differential equation to model the internal temperature of the battery, which is used to calculate the temperature effects on capacity and the degradation rate:

$$T_{i+1} = \left(T_i - T_a - \frac{\dot{Q}}{h}\right) e^{-\frac{h}{mc}dt} + \frac{\dot{Q}}{h} + T_a \tag{4-16}$$

where $T_i$ is the current internal temperature of the battery and $T_{i+1}$ is the temperature after the time $dt$ has elapsed [39].

Since the Modified Kinetic Battery Model allows for custom batteries to be created, the specifications for the Trojan battery was inputted into the model. Figure 13 depicts the exponential relationship between shelf-life versus temperature. As can be seen, the shelf-life of a battery is a decreasing convex function of temperature: as the temperature increases, the lifetime of the battery is reduced at a decreasing rate. HOMER applies a simplified Arrhenius equation to model this relationship:

$$k = \mu_1 \cdot e^{-\frac{\mu_2}{T_k}} \tag{4-17}$$

where $k$ is the rate of increase in degradation, $\mu_1$ and $\mu_2$ are fitted parameters, and $T_k$ is the temperature in Kelvin [39].

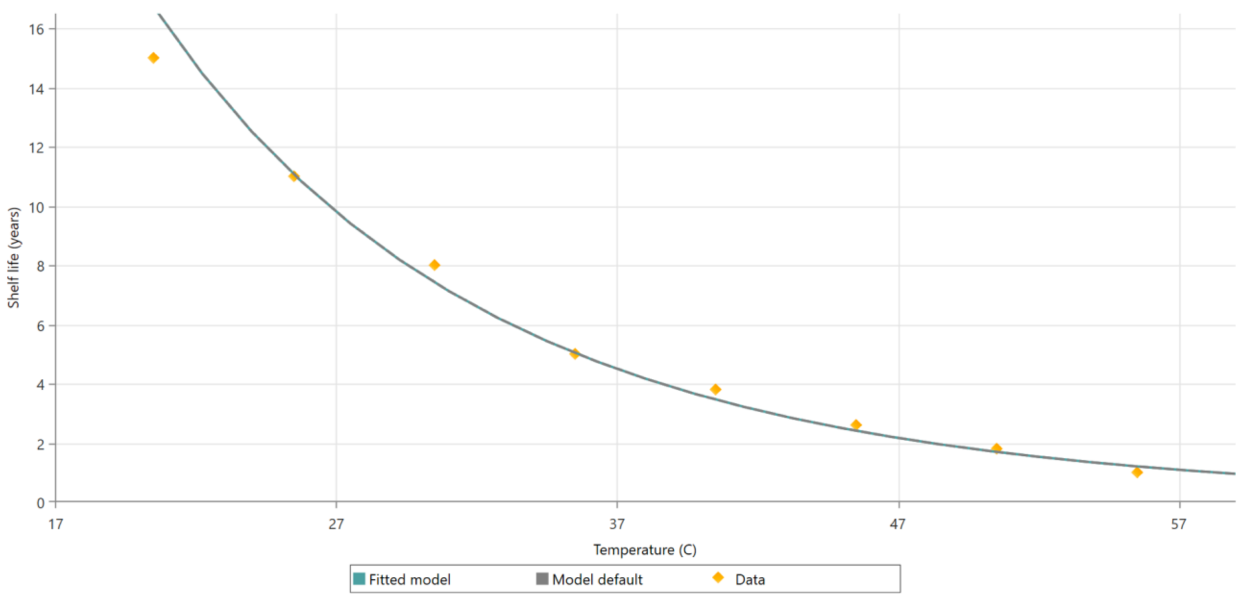


**Figure 13 Relationship between Shelf Life and Temperature**

In addition, the lifetime of the battery can also be reduced by nearly one third depending on how much the battery is depleted, as expressed by the exponential relationship that exists between number of battery cycles and depth of discharge (DOD) depicted in Figure 14. The *DOD = 1 – SOC* indicates the percentage of the capacity which has been removed from the fully charged battery. HOMER models this behavior as follows:

$$\frac{1}{N} = \alpha \cdot DOD^{\beta} \tag{4-18}$$

where $N$ is the number of cycles, and $\alpha$ and $\beta$ are fitted constants [39].

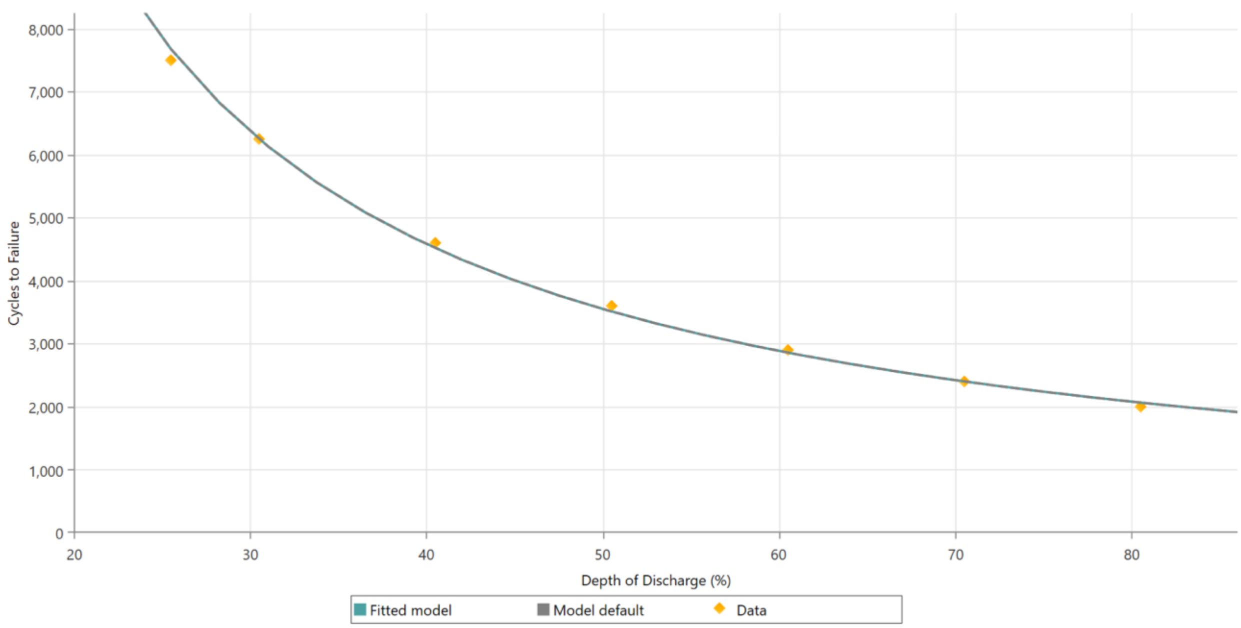


**Figure 14 Relationship between DOD and Cycles to Failure**

Furthermore, recognizing the second order polynomial relationship between temperature and relative battery capacity is important particularly for any techno-economic analysis. The battery will shut down outside of this temperature range, which is between -20°C and 45°C, as depicted in Figure 15. HOMER models this relationship as follows:

$$BC(T) = NBC \cdot (d_2 T_C^2 + d_1 T_C + d_0) \quad \text{(4-19)}$$

where *BC(T)* is the battery capacity as a function of temperature, *NBC* is the nominal battery capacity, $d_0$, $d_1$, and $d_2$ are fitted parameters based on the data available, and $T_C$ is the temperature in degrees Celsius [39].

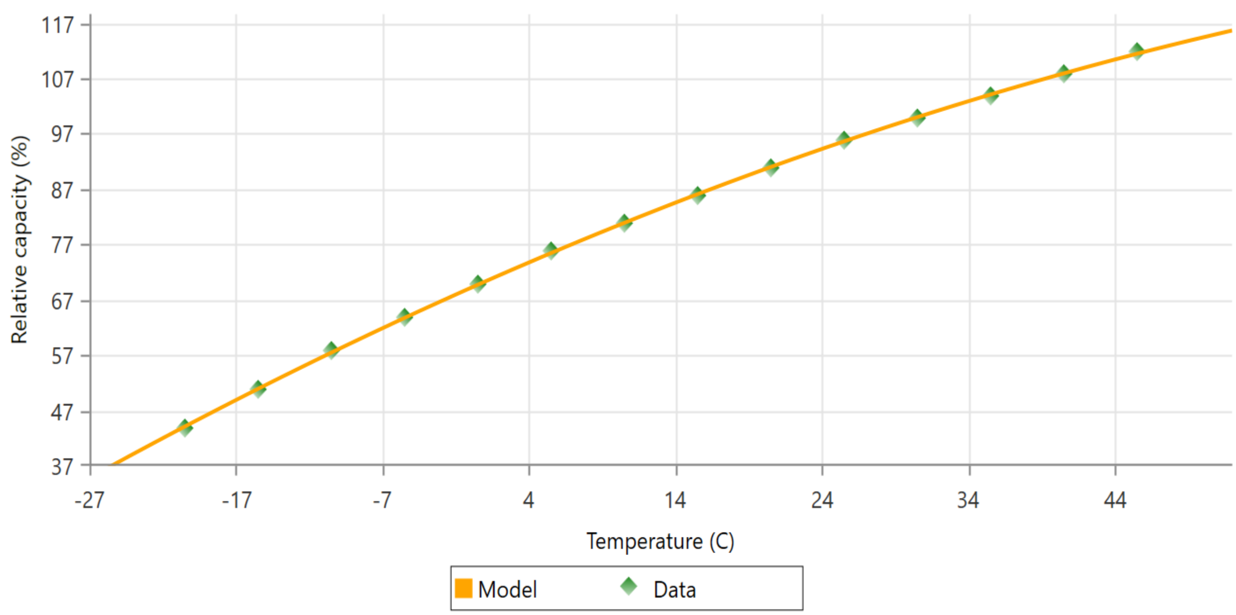


**Figure 15 Relationship between Temperature and Relative Capacity**

The dispatch strategy used the proposed system is the 'load following' strategy. Under this control strategy, HOMER dispatches the battery storage bank to serve the load when there is insufficient PV energy [39]. In order to analyze the relationship between temperature and battery lifetime and how it can impact the economics of the system, average monthly temperatures were inputted into HOMER (see Appendix B). Since this study considers three scenarios (optimistic, most likely, and pessimistic) the corresponding monthly temperatures were calculated based on the Navajo Nation's monthly average temperature data (2019) and were adjusted based on corresponding projected air temperature increases presented earlier in Table 1 in Section 4.1. Thus, the inputted monthly temperatures for the optimistic, most likely, and pessimistic simulations were 2°F, 4°F, and 6°F greater than the Navajo Nation's average 2019 monthly temperatures, respectively.

#### 4.2.3.2 Simulation Results

As discussed, battery life and performance are mainly dependent on temperature and how deep the batteries are discharged. In order to analyze the effects of these factors on the economics of the system, two sets of results are considered in this study for each of the three scenarios: *with* temperature effects and *without* temperature effects. All results are generated using HOMER's "Optimizer™" feature, which utilizes an algorithm to find the optimal system sizing with least NPC [39].

When considering *with* temperature effects, HOMER uses a lumped thermal model to simulate the battery bank's internal temperatures on capacity and lifetime [39]. Otherwise, when the simulation is ran *without* temperature effects considered, HOMER results are generated using a fixed internal temperature for the battery. As shown in Table 7, the simulated lifetime of the batteries is 17 years for the *without* temperature effects case, which is the OEM's specification. In contrast, in the *with* temperature effects case, the simulated lifetime of the batteries is significantly shorter and even a 1-year difference in each operating scenario is observed.

**Table 7 Summary of Simulation Results**

| | w/ Temperature Effects | | | | | w/o Temperature Effects | | | | |
|---|---|---|---|---|---|---|---|---|---|---|
| **Scenario** | **PV (kW)** | **Battery Storage (units)** | **Battery Life (years)** | **Battery Replacement Cost ($)** | **Battery NPC ($)** | **PV (kW)** | **Battery Storage (units)** | **Battery Life (years)** | **Battery Replacement Cost ($)** | **Battery NPC ($)** |
| Optimistic | 15.8 | 15 | 11 | 41,841 | 66,512 | 18.4 | 9 | 17 | 12,217 | 28,772 |
| Most Likely | 17.5 | 15 | 10 | 43,433 | 71,481 | 16.0 | 10 | 17 | 13,574 | 31,969 |
| Pessimistic | 13.9 | 15 | 9 | 44,961 | 76,719 | 16.1 | 10 | 17 | 13,574 | 31,969 |

The results for the *without* temperature effects case is relatively close to the quantitative results for PV capacity and number of required batteries (calculated in Section 4.2.2 and summarized in Table 6), which validates the simulation results with the quantitative results. Interestingly, in the *with* temperature effects case, the longest battery lifetime occurs under the *optimistic* scenario (lowest ambient temperatures), but is still 6 years (35%) shorter than the nominal lifetime of the battery of 17 years; under the *pessimistic* scenario, the expected battery lifetime is approximately 50% shorter. This reduced battery lifetime results in significantly higher battery replacement costs and, hence, increased battery NPCs due to faster capacity depletion. As expected, the pessimistic scenario results in the highest replacement cost and NPC for the batteries. On the other hand, in the *without* temperature effects case, the difference in the battery replacement and NPCs for each scenario is not as significant. Appendix C displays the full set of simulation results. The overall economic analysis of the proposed system will be discussed in more detail in the following section.

## 5.0 Economic Analysis

The fundamental question regarding any proposed project requiring capital investment is whether the investment is likely to be economically viable under uncertain changing conditions. In this section, the proposed system's costs are analyzed in order to better understand climate change's impact on the economics of the system.

### 5.1 Effects of Temperature on System Costs

As discussed in Section 4.0 and shown in Figure 8, the components that make up the proposed system include: battery storage, PV array, DC motor, water pump, charge controller, DC-DC converter, and water storage tank. Each of these components have a different service life, requiring replacement in order to ensure continuous system operation.

The number replacements associated with the system components, aside from the batteries and the PV panels that were simulated by HOMER, are determined by using each components lifetime and the 28,896 hours of operation in the 25-year lifetime of the system, discussed earlier in the technical assumptions (Section 4.2.1). Table 8 presents the results as well as the assumed O&M cost per hour of operation. This information is used to estimate the replacement and O&M costs needed to conduct the NPC analysis of the system.

**Table 8 Estimated Units of Replacements and O&M Costs for System Components**

| Component | Lifetime (years) | Lifetime (hours) | Replacements (units) | O&M ($/hour) |
|---|---|---|---|---|
| Water Pump | 15 | 131,400 | 1 | 0.01 |
| DC Motor | 1.1 | 10,000 | 3 | 0.02 |
| DC-DC Converter | 1.1 | 10,000 | 3 | 0.02 |
| Charge Controller | 15 | 131,400 | 1 | 0 |
| Water Storage | 50 | 438,000 | 0 | 0.005 |
| PV | 25 | 219,000 | HOMER Results | 0.13 |
| Battery Storage | HOMER Results | HOMER Results | HOMER Results | 0.01 |

Tables 9 and 10 present the systems costs under the *pessimistic* (worst-case) scenario for the *with* and *without* temperature effects cases. Both tables include estimated initial capital, replacement, O&M, and salvage costs used for determining the NPC. Aside from the costs associated with the system components, the other costs included are 'installation and related services' (*e.g.*, training and site preparation) and 'other balance of system (BOS)' costs (*e.g.*, cables, safety equipment, meters and instrumentation). The 'other BOS' costs can account for 15% of total capital costs and 'installation and related services' can account for 25% [10]. The capital cost for the water storage tank is determined using the calculated water tank volume of 27,390 gallons at a rate of $0.3/gallon.

**Table 9 System Costs under Pessimistic Scenario – w/ Temperature Effects**

| Component | Capital | Replacement | O&M | Salvage | NPC |
|---|---|---|---|---|---|
| Battery Storage | $33,075 | $44,961 | $2,629 | -$3,947 | $76,718 |
| PV | $15,419 | $0 | $2,435 | $0 | $17,854 |
| DC Motor | $2,000 | $6,000 | $578 | $0 | $8,578 |
| Water Pump/Accessories | $800 | $800 | $289 | $0 | $1,889 |
| Charge Controller | $750 | $750 | $0 | $0 | $1,500 |
| DC-DC Converter | $500 | $1,500 | $0 | $0 | $2,000 |
| Water Storage | $8,217 | $0 | $1,095 | $0 | $9,312 |
| Other BOS | 15% | $0 | $0 | $0 | $9,114 |
| Installation/Services | 25% | $0 | $0 | $0 | $15,190 |
| 1 System | $85,065 | $54,011 | $7,026 | -$3,947 | $142,155 |
| 10 Systems | $850,654 | $540,110 | $70,259 | -$39,470 | **$1,421,553** |

**Table 10 System Costs under Pessimistic Scenario – w/o Temperature Effects**

| Component | Capital | Replacement | O&M | Salvage | NPC |
|---|---|---|---|---|---|
| Battery Storage | $22,050 | $13,574 | $1,753 | -$5,407 | $31,969 |
| PV | $17,846 | $0 | $2,818 | $0 | $20,664 |
| DC Motor | $2,000 | $6,000 | $578 | $0 | $8,578 |
| Water Pump/Accessories | $800 | $800 | $289 | $0 | $1,889 |
| Charge Controller | $750 | $750 | $0 | $0 | $1,500 |
| DC-DC Converter | $500 | $1,500 | $0 | $0 | $2,000 |
| Water Storage | $8,217 | $0 | $1,095 | $0 | $9,312 |
| Other BOS | 15% | $0 | $0 | $0 | $7,824 |
| Installation/Services | 25% | $0 | $0 | $0 | $13,041 |
| 1 System | $73,028 | $22,624 | $6,533 | -$5,407 | $96,777 |
| 10 Systems | $730,282 | $226,240 | $65,327 | -$54,070 | **$967,771** |

While the capital and O&M costs for the two cases are not significantly different, the same cannot be said about the battery replacement costs. The battery storage component has the highest impact on the NPC between the two cases and the estimated battery replacement cost increases from $13,574 to $44,961, which represents over 3-fold increase. Under the ideal setting, where temperature effects on battery life is not a concern, the battery replacement cost of $13,574 constitutes 14% of the NPC per system. However, under the realistic condition of temperature effects, the battery replacement cost of $44,961 constitutes 32% of the NPC per system. The substantial increase in battery replacement costs and the resulting 1.5-fold increase on the overall NPC of the system is of paramount importance for the purpose of this study.

To extend the analysis beyond just the worst-case scenario, Table 11 is developed using the mean values from of the battery storage sizing and costing results for all three scenarios for comparison (see Appendix C). The mean of the probability distribution for the three-estimate (optimistic, most likely, pessimistic) approach, is determined as follows [30]:

$$Mean = \frac{O + 4M + P}{6} \tag{5-1}$$

The table presents the mean values for battery life, initial battery bank size, number of battery replacements, total number of batteries required throughout the system lifetime, initial capital costs, replacement costs, and net present cost for the batteries. Note that the total number of batteries required is the sum of the initial battery bank size and number of battery replacements.

**Table 11 Battery Storage Sizing and Costs (Mean Values)**

| Battery Storage | w/o Temp. Effects | w/ Temp. Effects | % Increase |
|---|---|---|---|
| Life | 17 | 10 | -41% |
| Initial Sizing | 10 | 15 | 53% |
| Replacements | 6 | 20 | 231% |
| Total Batteries | 16 | 35 | 120% |
| Capital Cost | $21,315 | $33,075 | 55% |
| Replacement Cost | $13,122 | $43,422 | 231% |
| NPC | $30,903 | $71,526 | 131% |

The results indicate that even when considering the mean estimates (expected values), the life of the batteries is 41% shorter, resulting in a 131% increase in battery replacements, and hence expected 55% increase in battery capital cost, 231% increase replacement cost, and 131% increase in the overall NPC for the batteries. From the aforementioned analysis, the following generalization can be inferred: The battery sizing and costs for any off-grid microgrid system with lead acid battery storage will be significantly higher under the current environment of the warming climate. This effect will further be exacerbated in the hot climate regions where communities, like the ones in the Navajo Nation, are residing.

### 5.2 PV-Diesel vs. PV-Battery Systems

As mentioned previously, rapid cost decreases in electrochemical energy storage, such as batteries, have increased competition with conventional fuel alternatives. For this study, the lead acid batteries are replaced with a diesel generator to compare the economics of energy storage in the form of fuel instead of battery chemistry. As reported by NREL (2019), generator capital costs are about \$800/kW and O&M costs are about \$0.1/operating hour [40]. The lifetime of the generator is assumed to be 15,000 hours, with maintenance intervals every 400 hours of operation and \$25 of associated maintenance costs. Based on the average diesel fuel prices reported by U.S. Energy Information Administration, a fuel price of \$0.7/L is used for this analysis [41]. The assumptions for the diesel generator are listed in Table 12 and were inputted in the HOMER simulation.

**Table 12 Assumptions for Diesel Generator**

| Parameter | Value |
|---|---|
| Capital Cost | \$800/kW |
| Replacement Cost | \$800/kW |
| O&M Cost | \$0.1/operating hour |
| Fuel Price | \$0.7/L |
| Lifetime of Generator | 15,000 hours |
| Maintenance Intervals | every 400 hours of operation |
| Maintenance Cost | \$25 |

Table 13 and Figure 16 illustrate the cost comparison between the two energy storage alternatives considered for this study: diesel and lead acid batteries. It is clear that capital and replacement costs of the lead acid batteries is higher than for the diesel generator making diesel seem to be more economical. However, there is a substantial cost difference between the systems when considering the operating costs, such as O&M, fuel, and the overall NPCs for each.

**Table 13 Cost Summary of Energy Storage Alternatives**

| | Energy Storage | |
|---|---|---|
| **Cost** | **Diesel Generator** | **Lead Acid Battery** |
| Capital | $2,560 | $33,075 |
| Replacement | $12,548 | $44,961 |
| O&M | $88,007 | $2,629 |
| Fuel | $23,174 | $0 |
| NPC | $126,003 | $76,718 |

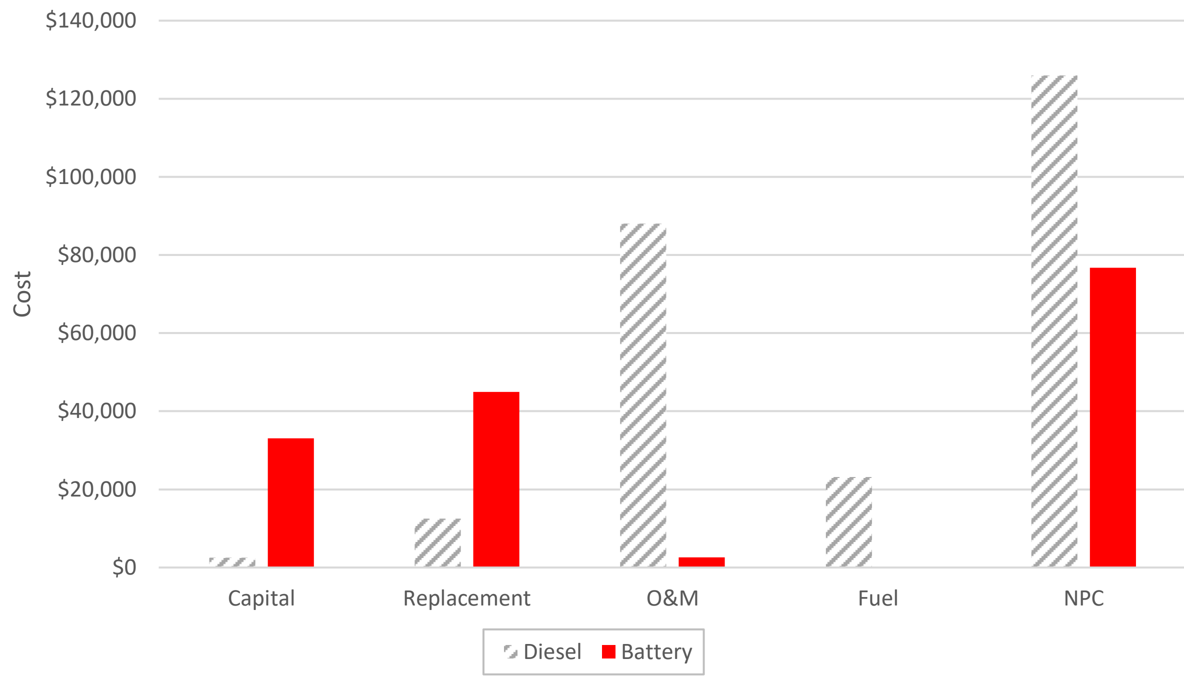


**Figure 16 Cost Comparison between Energy Storage Alternatives**

As can be seen, the diesel generator has significantly higher O&M costs, with a cost difference of about $90,000 which is approximately 34-fold higher than the O&M costs for the lead acid batteries. Further, battery energy storage systems only rely on generated power to recharge, whereas a diesel generator relies on fuel to replenish itself. This difference in operation introduces a new cost parameter into the mix, which is fuel cost. This results in the diesel generator having significantly higher NPC costs, with a cost difference approximately 2-fold higher than the

NPC of the battery. Not only does diesel have substantially higher costs, but it also creates negative environmental side effects. From this analysis, the following generalization can be inferred: Energy storage in the form of lead acid batteries for an off-grid microgrid system is the superior choice over a diesel generator due to its long-term economic savings and environmental sustainability advantages.

## 6.0 Conclusion and Implications

This study addressed the primary issue that most homeowners in off-grid rural areas are not good candidates for centralized water systems because power line extension to low population dense areas is not economically viable due to the principle of economies of scale. Many people living in rural areas, like those in the Navajo Nation, must travel long distances to haul water back to their homes due to limited water access points. There are two alternatives to address the limited water access and hauling issue: (1) To extend public water systems to provide all individual homes with piped water, at substantial costs; or (2) To provide adequate number of water access points targeting specific areas and population points by utilizing off-grid microgrid technology. This second approach was the motivation for this study. A PV-battery microgrid system for water pumping was proposed and was compared to diesel as an alternative source for energy storage. Both systems were designed and were evaluated to meet the local loads of a small community in the Navajo Nation, the LeChee Chapter, as a prototype example that can be implemented in areas with similar socio-economic and environmental conditions.

Upon identifying the need for an economical and technologically feasible approach to confront the water access issues in hot rural areas and the emerging threat of the warming climate, this study designed and evaluated the performance of the microgrid system under the *optimistic*, *most likely*, and *pessimistic* climate change scenarios. The technical requirements for the system components and operation were identified, followed by a quantitative analysis that was performed for determining the required power output of the PV array and battery storage capacity. Utilizing HOMER Pro, a highly recognized techno-economic microgrid software developed by NREL, the Modified Kinetic Battery Model was used to simulate battery performance and lifetime for both *with* and *without* temperature effects cases. An economic analysis was performed in order to better understand the financial implications of the warming climate on the overall sizing and economics of off-grid microgrid systems with lead acid battery storage. The study further conducted a cost comparison with a diesel generator as an alternative for energy storage.

The findings indicated that the expected life of lead acid batteries is 41% shorter, resulting in significantly higher battery sizing and costs for any off-grid microgrid system with battery storage under the current environment of the warming climate. Aside from the negative environmental side effects that diesel generators produce, the findings also indicated that diesel as energy storage had substantially higher costs, with a cost difference approximately 2-fold higher than the NPC of the battery. In the final analysis, this research reinforced that energy storage in the form of batteries for an off-grid microgrid system is the superior choice over a diesel generator due to its long-term economic savings and environmental sustainability advantages. Thus, given the limited tribal resources, federal budgets, and authorizations, PV-battery systems for water pumping is more economical and environmentally advantageous for low-income rural communities, like the LeChee Chapter in the Navajo Nation.

A key practical implication of the findings is that in order to increase the field applications of off-grid microgrids, especially in the areas that they are most needed, *i.e.*, hot-climate areas with poor economic conditions and infrastructure, scientific and technological efforts must be geared towards developing energy storage technologies that perform more economically under hot temperature conditions. From a theoretical perspective, this study showed how the decision sciences method of the 'three-point estimation' technique can be utilized to better predict performance of power systems for more effective planning under the conditions of uncertainty.

This study highlighted the importance of considering environmental and operating temperature conditions for power system design and their effects on life, sizing, and the economics of a system. Like any research study, there are a number of limitations that can be considered for future research. It would be interesting to further investigate the proposed system under the presence of heating, ventilation, and air conditions (HVAC) equipment and evaluate its effects on battery life and the overall economics of the system. It would also be interesting to evaluate and compare the performance and economics of the system using lithium-ion (Li-ion) batteries. In addition, this study can be enhanced by incorporating other capital and O&M costs such as water sanitation, well drilling/construction, and DC circuit protection in the overall system's cost analysis.

# Appendix A Solar Radiation Data

**Table 14 Solar Radiation Data for Navajo Nation**

| Solar Radiation for Flat-Plate Collectors Facing South at a Fixed Tilt (kWh/m$^2$/day) for Navajo Nation | | | | | | | | | | | | | |
|---|---|---|---|---|---|---|---|---|---|---|---|---|---|
| **Tilt** | **Jan** | **Feb** | **Mar** | **Apr** | **May** | **June** | **July** | **Aug** | **Sept** | **Oct** | **Nov** | **Dec** | **Annual** |
| **Latitude -15°** | 4.70 | 5.42 | 6.85 | 7.39 | 7.81 | 8.25 | 7.29 | 7.00 | 6.99 | 6.18 | 5.04 | 4.20 | **6.43** |
| **Latitude** | 5.47 | 6.05 | 7.17 | 7.23 | 7.27 | 7.47 | 6.71 | 6.75 | 7.17 | 6.77 | 5.83 | 4.95 | **6.57** |
| **Latitude +15°** | 5.91 | 6.32 | 7.08 | 6.68 | 6.37 | 6.37 | 5.84 | 6.15 | 6.93 | 6.95 | 6.26 | 5.4 | **6.36** |
| **90°** | 5.39 | 5.31 | 5.06 | 3.79 | 2.96 | 2.61 | 2.64 | 3.33 | 4.63 | 5.58 | 5.62 | 5.04 | **4.33** |

# Appendix B Projections of Monthly Temperatures

**Table 15 Projected Monthly Temperatures in Navajo Nation by 2050**

| Month | Optimistic | | Most Likely | | Pessimistic | |
|---|---|---|---|---|---|---|
| | °F | °C | °F | °C | °F | °C |
| **Jan** | 49.1 | 9.5 | 51.1 | 10.6 | 53.1 | 11.7 |
| **Feb** | 56.4 | 13.6 | 58.4 | 14.7 | 60.4 | 15.8 |
| **Mar** | 63.5 | 17.5 | 65.5 | 18.6 | 67.5 | 19.7 |
| **Apr** | 71.8 | 22.1 | 73.8 | 23.2 | 75.8 | 24.3 |
| **May** | 81.0 | 27.2 | 83.0 | 28.3 | 85.0 | 29.4 |
| **Jun** | 92.0 | 33.3 | 94.0 | 34.4 | 96.0 | 35.6 |
| **Jul** | 95.0 | 35.0 | 97.0 | 36.1 | 99.0 | 37.2 |
| **Aug** | 92.1 | 33.4 | 94.1 | 34.5 | 96.1 | 35.6 |
| **Sep** | 85.5 | 29.7 | 87.5 | 30.8 | 89.5 | 31.9 |
| **Oct** | 73.7 | 23.2 | 75.7 | 24.3 | 77.7 | 25.4 |
| **Nov** | 59.7 | 15.4 | 61.7 | 16.5 | 63.7 | 17.6 |
| **Dec** | 49.1 | 9.5 | 51.1 | 10.6 | 53.1 | 11.7 |
| **Annual** | 72.4 | 22.4 | 74.4 | 23.6 | 76.4 | 24.7 |

# Appendix C HOMER Pro Results

**Table 16 Summary of Simulation Results – w/ Temperature Effects**

| Scenario | PV (kW) | Battery Storage (units) | Battery Life (years) | Battery Replacements (units) | Total Batteries (units) | Battery Capital Cost ($) | Battery Replacement Cost ($) | Battery NPC ($) |
|---|---|---|---|---|---|---|---|---|
| Optimistic | 15.8 | 15 | 11 | 19 | 34 | 33,075 | 41,841 | 66,512 |
| Most Likely | 17.5 | 15 | 10 | 20 | 35 | 33,075 | 43,433 | 71,481 |
| Pessimistic | 13.9 | 15 | 9 | 20 | 35 | 33,075 | 44,961 | 76,719 |

**Table 17 Summary of Simulation Results - w/o Temperature Effects**

| Scenario | PV (kW) | Battery Storage (units) | Battery Life (years) | Battery Replacements (units) | Total Batteries (units) | Battery Capital Cost ($) | Battery Replacement Cost ($) | Battery NPC ($) |
|---|---|---|---|---|---|---|---|---|
| Optimistic | 18.4 | 9 | 17 | 6 | 15 | 19,845 | 12,217 | 28,772 |
| Most Likely | 16.0 | 10 | 17 | 6 | 16 | 22,050 | 13,574 | 31,969 |
| Pessimistic | 16.1 | 10 | 17 | 6 | 16 | 22,050 | 13,574 | 31,969 |

## Bibliography


[1] M. N. Naik, S. Chandel and R. Chandel, "Review of Solar Photovoltaic Water Pumping System Technology for Irrigation and Community Drinking Water Supplies," *Renewable and Sustainable Energy Reviews*, 2015.

[2] A. Khare and N. Economu, "Solar Water Pump Technology Roadmap," May 2019. [Online]. Available: https://efficiencyforaccess.org.

[3] A. Singh, "Techno-Economic Feasibility Study of Solar Water Pumping for Public Facilities in Nigeria," 2019.

[4] C. Scharp, J. G. Canuto and C. Cormency, "Scaling Up Solar Powered Water Supply Systems," 2016. [Online]. Available: https://www.unicef.org.

[5] "A Solar-Powered Solution to the Water Problem in Tanzania," World Bank Group, 2017. [Online]. Available: https://www.worldbank.org.

[6] Z. Roller, "Closing the Water Access Gap in the United States," DigDeep Right to Water Project, US Water Alliance, 2019.

[7] R. Salter, M. Dworkin, C. Gonzalez and R. Mastor, "Energy Access is Energy Justice," in *Energy Justice*, Edward Elgar Publishing, 2018.

[8] "Broken Promises: Continuing Federal Funding Shortfall for Native Americans," U.S. Commission on Civil Rights, Washington, DC, 2018.

[9] S. M. Larned, "Water is Life: The Native American Tribal Role in Protecting Natural Resources," *Environmental and Earth Law Journal*, vol. 8, 2018.

[10] "Solar Pumping: The Basics," International Bank for Reconstruction and Development/World Bank Group, Washington, DC, 2018.

[11] N. Argaw, "Renewable Energy in Water and Wastewater Treatment Applications," National Renewable Energy Laboratory, Golden, CO, 2003.

[12] A. Waeli and M. Khedr, "Optimum Design and Evaluation of Solar Water Pumping System for Rural Areas," *International Journal of Renewable Energy Research*, vol. 7, no. 1, 2017.

[13] "Colorado River Basin Ten Tribes Partnership Tribal Water Study Report," 2018. [Online]. Available: https://www.usbr.gov.

[14] "The American Indian and Alaska Native Population: 2010," 2012. [Online]. Available: https://www.census.gov.

[15] "Official Site of the Navajo Nation," Department of Information Technology, 2011. [Online]. Available: https://www.navajo-nsn.gov/history.htm.

[16] "Light Up the Navajo Nation," American Public Power Association, 2020. [Online]. Available: https://www.publicpower.org.

[17] "Providing Safe Drinking Water in Areas with Abandoned Uranium Mines," United States Environmental Protection Agency, 2020. [Online]. Available: https://www.epa.gov.

[18] "Navajo Nation Department of Water Resources," 2020. [Online]. Available: https://www.nndwr.navajo-nsn.gov.

[19] "Regional Water Plan for Tuba City Nine Chapters," Midvale, 2016.

[20] G. Garfin, A. Jardine, R. Merideth, M. Black and S. LeRoy, "Assessment of Climate Change in the Southwest United States: A Report Prepared for the National Climate Assessment," Island Press, Washington, DC, 2013.

[21] R. Frankson and K. Kunkel, "Arizona State Climate Summary," NOAA National Centers for Environmental Information, 2019.

[22] M. H. Redsteer and L. Amoroso, "More Heat, Less Water," U.S. Climate Resilience Toolkit, 2017. [Online]. Available: https://toolkit.climate.gov.

[23] J. Melilo, G. Yohe and T. Richmond, "Climate Change Impacts in the United States: The Third National Climate Assessment," U.S. Government Printing Office, Washington, DC, 2014.

[24] A. Layns, "Dramatic Decline in Lake Powell Water Levels," 2010. [Online]. Available: https://www.climate.gov.

[25] S.-H. Kim, Electric Motor Control, Seoul: Elsevier, 2016.

[26] N. Chandrasekaran and K. Thyagarajah, "Simulation and Experimental Validation of AC Motor and PMDC Motor Pumping System Fed by Photovoltaic Cell," *Journal of Engineering & Materials Science*, vol. 21, pp. 93-103, 2014.

[27] "Final Environmental Assessment: Water Service Contract Between the United States and The Navajo Nation / Navajo Tribal Utility Authority," U.S. Department of the Interior Bureau of Reclamation, Durango, CO, 2009.

[28] G. B. Gharehpetian and S. M. M. Agah, Distributed Generation Systems, Butterworth-Heinemann, 2017.

[29] W. Diao, Y. Xing, S. Saxena and M. Pecht, "Evaluation of Present Accelerated Temperature Testing and Modeling of Batteries," *Applied Sciences*, 2018.

[30] "Trojan Battery Company: Solar SIND 06 1225 Data Sheet," [Online]. Available: https://www.trojanbattery.com/pdf/datasheets/SIND_06_1225_DS.pdf.

[31] A. M. Elshurafa and M. H. Aldubyan, "State-of-Charge Effects on Standalone Solar-Storage Systems in Hot Climates," *Sustainability*, 2019.

[32] F. Hillier and G. Lieberman, Introduction to Operations Research, New York, NY: McGraw Hill, 2015.

[33] "My Tribal Area," The American Community Survey, 2018. [Online]. Available: https://www.census.gov.

[34] "Why Does the Federal Reserve Aim for Inflation of 2% Over the Longer Run?," Board of Governors of the Federal Reserve System, [Online]. Available: https://www.federalreserve.gov.

[35] T. D. Morales and J. Busch, "Design of Small Photovoltaic (PV) Solar-Powered Water Pump Systems," U.S. Department of Agriculture, Portland, OR, 2010.

[36] R. Fu, D. Feldman and R. Margolis, "U.S. Solar Photovoltaic System Cost Benchmark," National Renewable Energy Laboratory, 2018.

[37] "Solar Resource Data, Tools, and Maps," National Renewable Energy Laboratory, 2018. [Online]. Available: https://www.nrel.gov/gis/solar.html.

[38] E. Lockhart, X. Li, S. Booth, J. Salasovich, D. Olis, J. Elsworth and L. Lisell, "Comparative Study of Techno-Economics of Lithium-Ion and Lead Acid Batteries in Microgrids in Sub-Saharan Africa," National Renewable Energy Laboratory, 2019.

[39] "Help Manual," HOMER Energy, Boulder, CO, 2016.

[40] S. Ericson and D. Olis, "A Comparison of Fuel Choice for Backup Generators," National Renewable Energy Laboratory, Golden, CO, 2019.

[41] "Gasoline and Diesel Fuel Update," U.S. Energy Information Administration, 2020. [Online]. Available: https://www.eia.gov.